Cement & Concrete Composites 45 (2014) 166–175

Contents lists available at ScienceDirect

Cement & Concrete Composites

journal homepage: www.elsevier.com/locate/cemconcomp

Effects of phosphate on the chloride-induced corrosion behavior of reinforcing steel in mortars

J.J. Shi *, W. Sun

School of Materials Science and Engineering, Jiangsu Key Laboratory of Construction Materials, Southeast University, Nanjing 211189, China

ARTICLE INFO

Article history:
Received 30 August 2012
Received in revised form 16 September 2013
Accepted 2 October 2013
Available online 17 October 2013

Keywords:
Phosphate
Reinforcing steel
Mortar
Corrosion inhibition mechanism
Microstructure
Electrochemical methods

ABSTRACT

The influence of phosphate as a corrosion inhibitor on the corrosion behavior of as-received and pre-rusted reinforcing steels in mortar specimens was investigated after 360 days exposure in 3.5% NaCl solution. This involved the use of electrochemical techniques for studying the steel surface reactions and microscopic observations of the steel–mortar interface. The electrochemical methods, including electrochemical impedance spectroscopy (EIS) and measurements of corrosion potential (E_{corr}) and linear polarization resistance (LPR), were employed to evaluate the corrosion tendency and general corrosion rate of steel. In addition, the pitting corrosion resistance of steel was also determined by cyclic polarization (CP) measurements. The results indicate that different from nitrite, which is generally accepted as an anodic inhibitor, phosphate may be a cathodic inhibitor according to its reduced corrosion rate and more negative E_{corr} at the same dosage as nitrite in mortar specimens. The study also reveals that the inhibiting efficiency of phosphate against general corrosion of both as-received and pre-rusted specimens is lower than 10%, which is inferior to nitrite in some respects. However, as indicated by cyclic polarization measurements, the presence of phosphate provides slightly higher pitting corrosion resistance in comparison to nitrite. Furthermore, it suggests that the corrosion inhibition mechanism of phosphate in mortars mainly depends on a dual effect occurring at the steel–mortar interface. Furthermore, it is confirmed that phosphate has little effect on the long-term mechanical properties of mortars.

1. Introduction

One of the most important factors governing durability of reinforced concrete structures (RCS) is the chloride-induced corrosion of reinforcing steel, particularly in the coastal marine environment [1]. Numerous protection techniques have been employed to mitigate the corrosion risk, with respect to both the initiation and propagation stages of corrosion. Among them, the use of corrosion inhibitors has been considered as one of the most effective solutions [2–4,7–20].

Corrosion inhibitors are typically introduced either as an admixture during the mixing of fresh concrete [2–5] or as a surface application on the hardened concrete [7,8]. The migrating corrosion inhibitors, used for the latter approach, include sodium monofluoro-phosphate [7,8]. However, the efficiency of migrating corrosion inhibitors generally depends on the permeability of concrete [2].

As it has been previously reported, both inorganic and organic chemicals have been considered as corrosion inhibitors to use in RCS. Nitrite-based inhibitors, which are the typical inorganic inhibitor, have been applied effectively in RCS for a long period [2,3]. However, due to the possible toxicity of nitrites, their use for RCS corrosion protection has been forbidden in many countries [2]. Therefore, the investigation of new corrosion inhibitors is an urgent problem. Recently, nitrates (mainly calcium nitrate) have been proven to be a good alternative to nitrites because they are less harmful and more available [4,5]. The development of effective green inhibitors for applications within various severe environments is an important research objective.

At present, phosphate is one of the green inhibitors used for copper and copper alloy [6]. However, phosphate has seldom been studied as the corrosion inhibitor for steel, in particular for reinforcing steel in concrete in previous investigations [7–20]. These phosphate based inhibitors mainly include sodium monofluorophosphate (MFP: Na_2PO_3F) [7,8,20], sodium hydrogen phosphate (SHP: Na_2HPO_4) [9–11,20] and sodium phosphate (SP: Na_3PO_4) [12–20]. MFP has been widely investigated as a migrating corrosion inhibitor in chloride contaminated and carbonated concrete [7,8]. It has been reported that MFP may be rendered ineffective during the process of diffusion from the surface of concrete to the steel surface, due to its partial decomposition and precipitation in the cracks and pores of concrete [7]. Abd El Haleem et al. [10] studied the effect of HPO_4^{2-} on the pitting corrosion performance

* Corresponding author. Tel.: +86 25 52090667.
E-mail address: jinjies@126.com (J.J. Shi).

0958-9465/$ - see front matter © 2013 Elsevier Ltd. All rights reserved.
http://dx.doi.org/10.1016/j.cemconcomp.2013.10.002

of reinforcing steel in $Ca(OH)_2$ solution. The results revealed that the efficiency of pitting inhibition of HPO_4^{2-} was lower than NO_2^-. Moreover, in previous research by Jin et al. [11], it was demonstrated that HPO_4^{2-} (PO_4^{3-}) was much less stable than NO_2^- in cement paste according to linear polarization and corrosion potential measurements. Besides, HPO_4^{2-} was also found to inhibit the setting of cement.

Dhouibi et al. [12] compared the inhibiting effect of PO_4^{3-} and NO_2^- in saturated $Ca(OH)_2$ solution. The results from the electrochemical techniques showed that phosphate may be either a cathodic or anodic inhibitor, which normally depended on the concentration of inhibitor. In the later work of Dhouibi et al. [13], it was reported that phosphate can prevent pitting corrosion if its content was equal to chloride concentration. However, the results for the concrete specimens indicated that, after long-term (3 years) exposure in chloride solution, phosphate lost partially the effectiveness of corrosion inhibition. Recently, Etteyeb et al. [14–17] intensively studied the protection against corrosion for steel by pretreatment in phosphate solution before immersion in chloride solution. The results confirmed that the pretreatment contributed to the formation of a passive film on the steel surface, which reduced the corrosion rate of steel in saturated $Ca(OH)_2$ solution effectively. However, with regard to steel embedded in mortar specimens, the pretreatment against corrosion was somehow temporary [17].

The previous investigations of phosphate as the corrosion inhibitor of steel were mainly carried out in simulated concrete pore solutions (mainly saturated $Ca(OH)_2$). Therefore, tests for the effectiveness of phosphate used in mortar or concrete are relatively scarce, although the testing in mortar and concrete specimens has generally been considered to be more representative of the real conditions under which steel corrodes. In the present work, various electrochemical methods were performed to evaluate the corrosion behaviors of reinforcing steel in mortar specimens produced with phosphate or nitrite admixtures and exposed to 3.5% NaCl solution for 360 days. Moreover, the inhibiting efficiency of these two inorganic corrosion inhibitors on the corrosion rate of as-received and pre-rusted reinforcing steels was compared. Finally, the mechanism for phosphate in terms of preventing reinforcing steel from corrosion in mortar specimens was analyzed by a combination of electrochemical measurements and characterization of bulk microstructure of the steel–mortar interface.

2. Materials and methods

2.1. Specimen preparation

Small prismatic mortar specimens of 40 mm × 40 mm × 160 mm were cast. The mortar specimens were prepared with ordinary Portland cement (P·I 52.5). The fine aggregate used in this study was river sand with fineness modulus of 2.50. The cement/sand ratio (c/s) of 0.67 and water/cement ratio (w/c) of 0.53 were used for the mortar preparation. Round construction reinforcing steels with the diameter of 8 mm were embedded centrally in mortar specimens with the cover depth of 16 mm. A copper wire was soldered to one end of the reinforcing steel, and both ends were covered with epoxy resin coating, leaving a free exposure surface of approximately 20 cm^2.

To study the corrosion performance of pre-rusted reinforcing steels which are frequently used under field conditions, two surface conditions of reinforcing steels were investigated in this study: (1) pre-rusted reinforcing steel: the uniform thin corrosion products were formed on the surface of reinforcing steel after placing in humid atmospheric environment for 60 days, and (2) as-received reinforcing steel: without any surface modification.

The corrosion inhibitors, $NaNO_2$ (SN) and $Na_3PO_4{\cdot}12H_2O$ (SP), were added during mixing both with the content of 0.4 mol per 1 kg cement. The blank mortar specimens without corrosion inhibitor were also prepared for the comparative purpose. After 24 h casting, all specimens were curing (temperature = 20 ± 2 °C, and RH > 95%) for 28 days. Afterwards, the specimens were covered with epoxy resin coating again at both ends to avoid crevice corrosion. All the mortar specimens were exposed to 3.5% NaCl solution to accelerate the corrosion process. The immersion tests lasted for 360 days at room temperature (25 ± 1 °C).

2.2. Electrochemical and analytical methods

The corrosion potential (E_{corr}) and corrosion current density (i_{corr}) were monitored by means of linear polarization resistance (LPR) and electrochemical impedance spectroscopy (EIS). Cyclic polarization (CP) method was also used to evaluate the resistance to localized corrosion. A classical three-electrode arrangement was used for the electrochemical measurements, namely the reinforcing steel (working electrode), a stainless steel plate electrode (counter electrode) and a saturated calomel reference electrode (SCE), which were all connected to PARSTAT 2273 Potentiostat. In this study, all the potentials were relative to SCE.

In LPR tests, the reinforcing steels were polarized to ±10 mV vs E_{corr} with a scan rate of 0.166 mV/s. The *IR* potential compensation was adopted to eliminate the impact of the high resistivity of mortar matrix. EIS measurement was carried out at the corrosion potential with the scanning frequency ranged from 100 kHz to 10 mHz. The ac signal used in EIS was 10 mV. For CP testing, the potential polarization scanned from 100 mV more negative to E_{corr} of each specimen toward +800 mV and finally the potential was reversed to E_{corr}, with a constant scan rate of 1 mV/s. All the electrochemical tests were carried out at room temperature (25 ± 1 °C).

The photographs of surface topography of reinforcing steels in different conditions were compared after taking from the broken mortar specimens. Quanta 3D FEG environmental scanning electron microscopy (ESEM) was employed to obtain the microstructure variations of steel–mortar interface with and without inhibitors.

2.3. Mechanical properties testing

Flexural strength (three point bending test) and compressive strength of prismatic mortar specimens without reinforcing steels were tested both at early curing stage (28 days) and long-term exposure to atmospheric environment (360 days). The mechanical properties of mortar specimens in the presence of SN or SP were compared to the blank one. The dosages of SN and SP in mortar specimens were the same as in the electrochemical tests.

3. Results and discussion

3.1. Corrosion potential and polarization resistance

Fig. 1 shows the corrosion potential and polarization resistance of reinforcing steel with and without corrosion inhibitors after 360 days exposure in 3.5% NaCl solution. It can be seen from Fig. 1a that the E_{corr} values of all specimens are more negative than −400 mV_{SCE}, which is an indication of 90% probability of active corrosion as recommended in ASTM C876. The E_{corr} values of all pre-rusted reinforcing steels are slightly more negative than as-received ones, indicating that the pre-rusted steels exhibit higher probability of corrosion compared with as-received specimens. In addition, the E_{corr} values of blank specimens are much more negative than SN specimens and more noble than those with SP, both

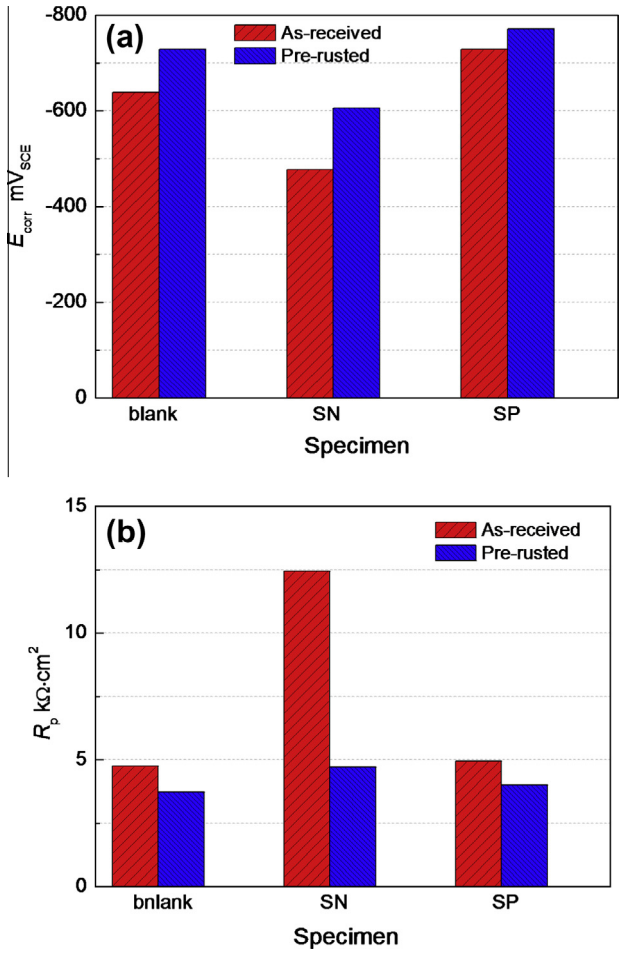

Fig. 1. The effect of inhibitors on the E_{corr} (a) and R_p (b) of reinforcing steel in mortar specimens after 360 days immersion.

for as-received and pre-rusted reinforcing steels. Generally, the more negative E_{corr} value indicates higher probability of depassivation for reinforcing steel. However, as given in a recent review [21], if the diffusion rate of oxygen increased in cracked concrete, more positive E_{corr} values and higher corrosion rates may be obtained. On the other hand, when the concrete samples were insulated from oxygen (saturated concrete or immersed in water), more negative E_{corr} values and lower corrosion rates were usually observed. Therefore, E_{corr} value should not be the single parameter to assess the electrochemical condition of reinforcing steel in cementitious materials, especially in the presence of inhibitors [5].

The results of polarization resistance are presented in Fig. 1b. It is evident that the R_p value of as-received reinforcing steel in SN specimen is approximately 12.5 kΩ cm^2, which is significantly higher than the blank and SP specimens. Moreover, the R_p value of SP specimen is merely slightly higher than blank specimen, suggesting that SN exhibits better inhibiting efficiency than SP at the same concentration in as-received mortar specimens. However, the R_p values for all pre-rusted reinforcing steels are lower than 5 kΩ cm^2, indicating higher corrosion rates are obtained for the pre-rusted reinforcing steels. As is well known, R_p value is inversely proportional to the corrosion rate of reinforcing steel. The lower R_p values of pre-rusted reinforcing steels indicate that, SN and SP in this study cannot effectively repassivate the pre-rusted reinforcing steel. However, both inhibitors are capable of restraining the propagation of corrosion to some extent.

According to the different protection mechanisms, corrosion inhibitor can be divided into three types [2,22]: (1) anodic zinhibitors, which are able to reduce the corrosion rate by an increase in E_{corr} value. (2) Cathodic inhibitors, which delay the diffusion of oxygen, thus reducing the corrosion rate by more negative E_{corr} value. (3) The mixed inhibitors, which affect both the anodic and cathodic reactions of corrosion thereby reducing the corrosion rate with no obvious change in E_{corr} value.

The effect of anodic and cathodic inhibitors on the corrosion state of reinforcing steel can be shown in Fig. 2. As indicated in Fig. 1, SN can reduce the corrosion rate with more noble E_{corr} value, whereas SP also results in the decreasing corrosion rate but with more negative E_{corr} value. Therefore, it is clear that SN is an anodic inhibitor while SP might be a cathodic inhibitor, according to the theory presented in Fig. 2. It has been previously reported [2,23] that, phosphate acted as a cathodic inhibitor due to the formation of a film on the surface of steel electrode. Moreover, it was found that, when the concentration of phosphates was lower than chlorides, sodium phosphate was thought to act as a cathodic inhibitor [12,13]. In contrast, at sufficiently high concentration, sodium phosphate was more likely to serve as a mixed inhibitor [13] or an anodic inhibitor [12]. In addition, it was also detected that sodium phosphate may be an anodic inhibitor in the presence of chloride ions and oxygen [15,18,24].

3.2. Electrochemical impendence spectroscopy

Fig. 3 shows the Nyquist plots of impedance spectra for reinforcing steel. As can be seen in Fig. 3, all the Nyquist plots present two capacitive loops (semi-circle arcs). The high frequency domain shows a small partial semi-circle arc which is related with the dielectric properties of mortar (time constant R_cC_c), whereas the low frequency domain displays part of large semicircle arc which deals with the electrochemical reaction on the steel surface (time constant $R_{ct}Q_{dl}$). The depressed semi-circles in Fig. 3 suggest a non-ideal behavior of double layer capacitance (C_{dl}) on the steel–mortar interface [25]. Therefore, C_{dl} is replaced by constant phase element (CPE) Q_{dl}. In general, the diameter of low frequency capacitive arc is equal to the charge transfer resistance R_{ct}. Hence the larger diameter is, the greater the R_{ct}, and the lower the corrosion current density i_{corr} are. It is interesting to find the presence of low frequency tails (a diagonal line with a slope of about 45°) for both as-received and pre-rusted specimens when SN was added. As previously reported [25–27], the low frequency tails may be the occurrence of Warburg impedance W. In EIS tests, the impedance of W can be given in the following equation:

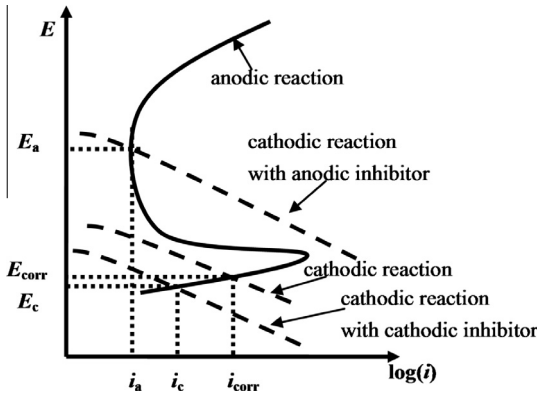

Fig. 2. Schematic illustration of the effect of anodic and cathodic inhibitors on corrosion potential (E_{corr}) and corrosion current density (i_{corr}) of reinforcing steel [22] E_a and i_a are corrosion potential and corrosion current density for reinforcing steel with anodic inhibitor, respectively; E_c and i_c are corrosion potential and corrosion current density for reinforcing steel with cathodic inhibitor, respectively.

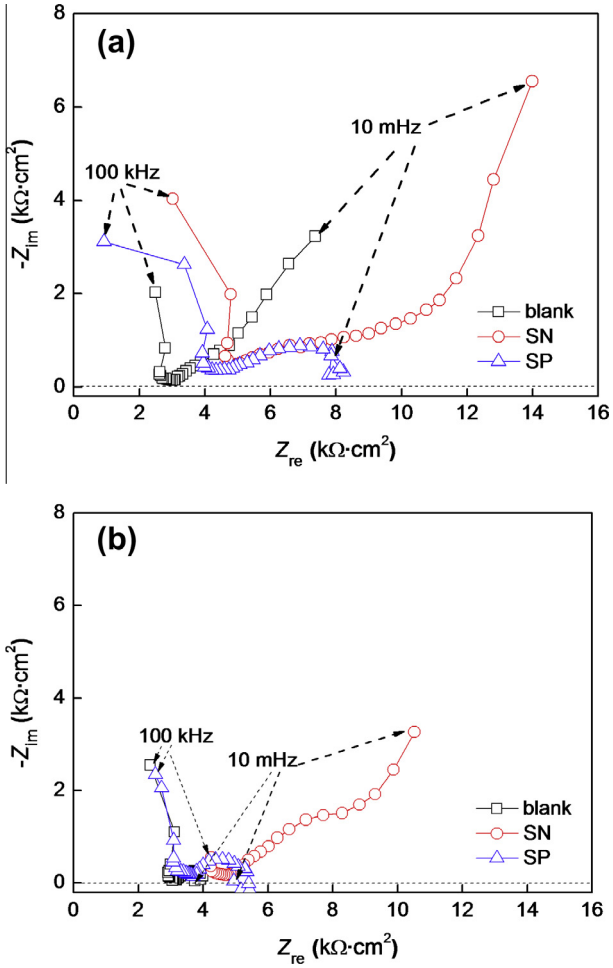

Fig. 3. Nyquist plots for reinforcing steel in mortar specimens with and without inhibitors exposed in 3.5% NaCl solution for 360 days. (a) As-received and (b) pre-rusted.

$$Z_W = \sigma_W(\omega)^{-1/2}(1-j) \quad (1)$$

where σ_W is the Warburg coefficient and ω is the angular frequency [26]. According to the work of Eichler et al. [27], Warburg impedance represented a diffusion process of oxygen for passive steel in simulated concrete pore solution. When corrosion products were observed on the steel surface, Warburg impedance was related with the diffusion of dissolved oxidants. It is confirmed that the presence of Warburg impedance in SN specimens is an indication of depassivation of reinforcing steel because no visible corrosion products can be observed on the steel surface. The control steps for the electrode reaction of steel are likely to change from the single charge transfer to a combination of charge transfer and oxygen diffusion. However, in the process of corrosion propagation (blank and SP specimens), Warburg impedance was not found in Nyquist plots.

Based on the properties of capacitive loops, equivalent circuits with two time constants were proposed to fit the electrochemical impedance spectra as shown in Fig. 4 [28]. The blank and SP specimens are fitted by the equivalent circuit presented in Fig. 4a. The SN specimen is fitted by the equivalent circuit with Warburg impedance as given in Fig. 4b. In these equivalent circuits, R_s is the resistance of solution used for electrochemical measurements. The first time constant (R_cC_c) is attributed to the high frequency response from mortar matrix, relating with the pore network and hydration products of cement [29]. The second time constant ($R_{ct}C_{dl}$) is related to the electrochemical reaction on the steel

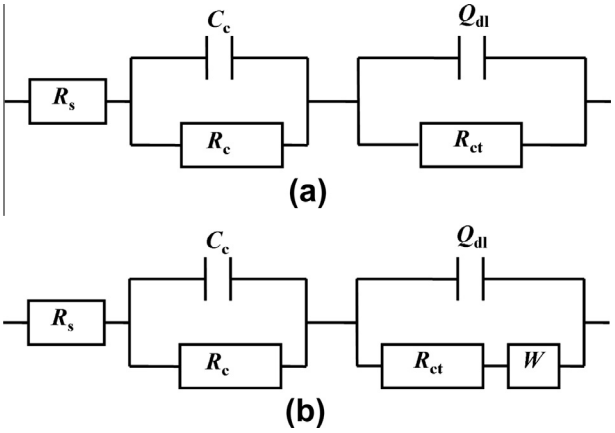

Fig. 4. The equivalent circuits used to fit the EIS data.

surface. R_{ct} is the charge transfer resistance of reinforcing steel, and Q_{dl} is the constant phase element (CPE) related with double layer capacitance (C_{dl}) on the steel–mortar interface. W in series with R_{ct} is the Warburg impedance. Vedalakshmi et al. [28] revealed that the former equivalent circuit in Fig. 4a was used to depict the steel under passive or uniform corrosion. However, the latter one shown in Fig. 4b with Warburg impedance is usually representative of steel under the condition of corrosion initiation.

The results of R_{ct} values fitted by ZSimpWin software are shown in Table 1. In the case of as-received reinforcing steels, it is clear that R_{ct} value of SN specimen is close to 12 kΩ cm^2, which is significantly higher than SP (4.89 kΩ cm^2) and blank (4.44 kΩ cm^2) specimens. As previously mentioned in Fig. 1b for pre-rusted reinforcing steels, the R_{ct} values of SN and SP specimens are merely slightly higher than that of blank specimens. The results suggest that neither SN nor SP is capable of pre-passivating the steel if corrosion products were previously formed on the steel surface. However, it must also be underlined that, in comparison to the as-received reinforcing steels, the condition of pre-rust herein does not exhibit extraordinary higher corrosion rate in high alkaline pore solution of cementitious materials.

Table 1 also lists the R_p values measured by LPR, with a comparison to the R_{ct} values. Apparently, R_p values are slightly higher than R_{ct} values in all cases, which is in good agreement with the previous investigations [14,29]. It was suggested in the study of Etteyeb et al. [14] that the simultaneous redox process with redox resistance R_{ox} occurring on the passive layer of steel surface was measured in LPR method, as given in Eq. (2). In addition, Koleva et al. [29] also reported that for corroding specimens, R_p may be equal to R_{ct} only if there were no mass transport processes. When transformations of the corrosion products emerged (resistance in the

Table 1
The polarization resistance and inhibiting efficiency of SN and SP measured by EIS and LPR.

Specimen	R_{ct} (EIS) (kΩ cm^2)	η (EIS) (%)	R_p (LPR) (kΩ cm^2)	η (LPR) (%)
As-received				
Blank	4.44	–	4.76	–
SN	11.99	63.0	12.43	61.7
SP	4.89	9.2	4.94	3.6
Pre-rusted				
Blank	3.22	–	3.72	–
SN	4.50	28.5	4.73	21.4
SP	3.94	18.3	4.02	7.5

corrosion product layer, denoted as R_{red}), R_p was in good agreement with the sum of R_{ct} and R_{red}.

$$R_p = R_{ct} + R_{ox} \quad (2)$$

On the contrary, Pradhan et al. [30] reported that the R_p values obtained by LPR were lower than R_{ct} measured by EIS in all concrete specimens, and a strong linear correlation existed between the i_{corr} values measured by these two methods as indicated by Eq. (3) with a regression coefficient of 0.994

$$i_{corr}(\mathrm{LPR}) = 1.10 \times i_{corr}(\mathrm{EIS}) \quad (3)$$

Similarly, as investigated in simulated concrete pore solution, Ghods et al. [31] also found that the values of polarization resistances obtained from EIS were generally higher than those from LPR. Therefore, a strong correlation existed as expressed in Eq. (4) with a regression coefficient of 0.97

$$\ln(R_p) = 0.90 \times \ln(R_{ct}) + 0.31 \quad (4)$$

In general, it would be reasonable to assume that this discrepancy may be attributed to the limitation of very time-consuming minimum frequency (a few mHz) test which is extraordinary important for the calculation of R_{ct} values in EIS. Moreover, it is inferred that the selection of a proper equivalent circuit for data fitting also plays a pronounced role on the R_{ct} values. Furthermore, the underlying pitfalls of LPR method, such as the imperfect compensation of *IR* potential drop due to the high resistivity of mortar matrix and/or the inappropriate scan rate, may also result in the inaccurate R_p values (underestimate or overestimate the true polarization resistance).

The inhibiting efficiency (η) of SN and SP for 360 days exposure is calculated by Eq. (5), as given in Table 1[16]:

$$\eta\ (\%) = \left[\frac{R_p(R_{ct}) - R_p^0(R_{ct}^0)}{R_p(R_{ct})}\right] \times 100 \quad (5)$$

where $R_p(R_{ct})$ and $R_p^0(R_{ct}^0)$ are the polarization resistances (charge transfer resistances) for inhibited and blank specimens, respectively. It is apparent that η values of SN are much higher than SP, especially in the case of as-received steel. Furthermore, SN exhibits much higher inhibiting efficiency for as-received steel than pre-rusted steel. It is also worth noting that, the inhibiting efficiency of SP in the condition of pre-rusted steel is interestingly higher than the as-received one. It is assumed to be attributed to the $Ca_3(PO_4)_2$ precipitate formed on the porous corrosion products, thus effectively preventing the propagation of corrosion of pre-rusted steel.

From the above results, it is reasonable to confirm that, if at the same concentration by the weight of cement, nitrite tends to be more effective in reducing the uniform corrosion rate of as-received reinforcing steel than phosphate after long-term exposure. It was generally believed that PO_4^{3-}, the effective constituent of this inhibitor, depleted partially due to the formation of precipitates by the reaction between Ca^{2+} and PO_4^{3-} when phosphates were added during mixing stage [7]. This may be one of the reasons of partially losing its efficiency when added directly into concrete [13]. However, one should bear in mind that, the effective inhibiting efficiency for admixed phosphate in simulating solutions and cementitious materials may be primarily dependent on the concentration of inhibitor as well as exposure time with inhibitor in aggressive environment [12,13].

More recently, it was well recognized that pretreatment (prepassivation) of steel in solution containing phosphates before exposure to aggressive solutions favored the formation of a protective passive film on the steel surface, and then higher inhibiting efficiency was obtained [16]. However, in mortar specimens, the effect of pretreatment was reported to be temporary [17].

It should also be noted that η values in this work were comparatively lower than that reported in the literature when tested in alkaline chloride media [16]. Generally, the inhibiting efficiency of inhibitors mainly depends on the bulk matrix (simulated concrete solution or mortar/concrete specimens), dosage of inhibitor and exposure time, etc. The presence of the porous steel–mortar interface is also considered as a dominating parameter affecting the corrosion behaviors and inhibiting efficiency as well. It is suggested that the accumulation of abundant chloride ions in the steel–mortar interface during a long period may exceed the content of SP. Consequently, it may be treated as the other possible reason for the partially lost of the effectiveness of phosphate in concrete after long-term exposure [13]. Therefore, the inhibiting efficiency of SP in reinforced mortar specimens after long-term exposure to NaCl solution was significantly lower than short-term tests for steel electrodes immersed directly in simulating solutions.

3.3. Cyclic polarization

The potentiodynamic cyclic polarization test is a relatively fast electrochemical method which allows providing information on pitting corrosion behavior of reinforcing steel. In general, we can obtain corrosion potential (E_{corr}), pitting potential (E_{pit}), repassivation potential (E_{rep}), passivation current density (i_{pass}) and maximum current density (i_{max}) from the cyclic polarization curves [32].

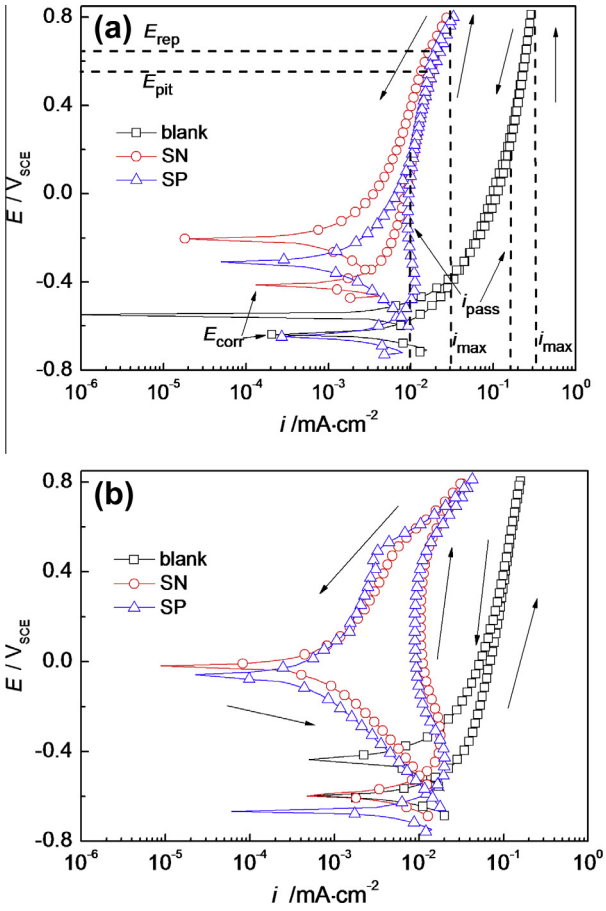

Fig. 5. Cyclic polarization curves for reinforcing steel in mortar specimens with and without inhibitors exposed in 3.5% NaCl solution for 360 days. (a) As-received and (b) pre-rusted.

Fig. 5 shows the cyclic polarization curves for as-received and pre-rusted reinforcing steels in mortar specimens with and without inhibitors at the end of immersion test. The relevant electrochemical parameters obtained from Fig. 5 are given in Table 2. It is suggested that no sharp increase in current density was detected in the process of potentiodynamic anodic polarization both for as-received and pre-rusted reinforcing steels in blank specimens, thus no distinct E_{pit} values could be obtained. This is consistent with the results found by Alonso-Falleiros et al. [33], which indicated that potentiostatic test appeared to be more reliable to determine the E_{pit} values than potentiodynamic test. Furthermore, Poursaee et al. [21] suggested that an appropriate cyclic polarization scan rate for the accurate reflection of the corrosion behavior was obligatory. Otherwise, different E_{pit} and E_{rep} values may be detected for the same specimen at different scan rates. As can be seen in Fig. 5, it is clear that the shape of curves for SN and SP specimens exhibit almost the same trend, except for the corrosion potential. However, the blank specimens exhibit dissimilarity in the curve shape with higher i_{pass} value, this consequently resulting in different pitting corrosion resistances.

In the work of Saremi et al. [32], i_{pass} was a criterion of anodic dissolution of reinforcing steel in passive state, and i_{max} indicated the rate of anodic dissolution of reinforcing steel within the corrosion pits. The as-received blank specimen exhibits much higher i_{pass} and i_{max} values than SN and SP specimens as shown in Fig. 5a, suggesting both SN and SP could effectively restrict the development of corrosion pits. This case is almost the same for pre-rusted specimens (Fig. 5b). However, it is interesting to find that the i_{pass} and i_{max} values of pre-rusted steels are lower than the as-received ones in blank specimen. It is believed to be associated with the possible uniform rust layer on the pre-rusted steel, which prevents the evolution of pitting corrosion.

As discussed above, it is sometimes difficult to determine the pitting resistance of reinforcing steel in the presence of SN or SP merely concerning E_{pit} or E_{rep} values. Therefore, the difference between different characteristic potentials as a criterion of pitting corrosion has been proposed widely as shown in Table 3 [32,35–36]. Saremi et al. [32] considered that ΔE_1 (difference between E_{pit} and E_{rep}) was related to the dissolution rate of the steel in the pits. It was generally admitted that the higher the ΔE_1, the lower the pitting corrosion resistance. It can be seen from Table 3, however, the ΔE_1 for all specimens were negative, indicating the absence of typical pitting corrosion [32,34]. Consequently, the pitting resistance could not be determined directly by ΔE_1. Troconis de Rincon et al. [35] used ΔE_2 (difference between E_{rep} and E_{corr}) as the criterion, and suggested that the higher the ΔE_2, the lower the probability of pitting corrosion. Furthermore, in the study of corrosion performance of new stainless steels, García-Alonso et al. [36] also proposed that ΔE_3 (difference between E_{pit} and E_{corr}) may reflect the pitting corrosion, indicating the higher the ΔE_3, the lower the probability to pitting corrosion. It is evident that both ΔE_2 and ΔE_3 of SP specimens are higher than those of SN specimens, regardless of the initial surface conditions. Thus, the results indicate that phosphate possesses lower probability to pitting corrosion compared with nitrite. The results herein are in good accordance with that reported in the literature [18,37]. Refaey et al. [37] found that PO_4^{3-} had a strong inhibitive effect of chloride induced pitting corrosion, and Génin et al. [18] also detected that the pitting potential became more noble in the presence of phosphate. On the contrary, Abd El Haleem et al. [10] found that the efficiency of pitting inhibition of HPO_4^{2-} was lower than NO_2^-. This inconsistency may be due to the different electrochemical methods used and different alkaline media tested (pH value and chlorides, etc.).

It can also be obtained from Table 3 that the probability to pitting corrosion is nearly the same for both surface conditions of steel, which may be attributed to the uniform corrosion products and white deposits formed on the surface of pre-rusted steel, thus inhibiting the further attack of chlorides to some extent.

3.4. Corrosion pattern of reinforcing steel

At the end of immersion tests, mortar specimens were split to allow visual inspection of steel surface. Fig. 6 presents the surface corrosion morphology of reinforcing steels. It is evident that red rust (Fe_2O_3 or hydrated Fe_2O_3) and green rust stains were observed on the steel surface for blank specimens, reflecting that the steels are severely corroded. The green rusts may be low valent oxides of iron or chloride-induced $Fe_4^{2+}Fe_2^{3+}(OH)_{12}(Cl,OH)_2$ [38] or $Fe_3^{2+}Fe^{3+}(OH)_8Cl$ [39]. As suggested by Koleva et al. [39], in the condition of poor oxygen supply, such as the specimens immersed completely in NaCl solution, black rust (Fe_3O_4) might be formed on the steel surface, which was also presented in the pre-rusted blank specimen in Fig. 6. With regard to the specimens with SN, scarcely any macroscopic corrosion products could be observed. In the presence of SP, as-received reinforcing steel exhibits a few local corrosion products. However, the surface of pre-rusted steel appears relatively smooth and homogeneous with no visible colored rusts. It is interesting to find that the pre-rusted steels in SP and SN specimens were covered with a calcium-rich layer (mainly white deposits in the form of $Ca(OH)_2$, $CaCO_3$ and/or $Ca_3(PO_4)_2$), indicating that a spot of uniform corrosion products may not result in corrosion propagation in cementitious materials up to 1 year [40]. The results of surface morphology of steel in different conditions are in good agreement with the results of electrochemical tests in this study.

3.5. Micrograph of reinforcing steel–mortar interface

Although there is strong evidence that the reduced corrosion rate of reinforcing steel in the presence of inhibitors is mainly attributed to the competitive surface adsorption between inhibitors and chloride ions or to the formation of protective film on the steel surface [2]. It is also well established that inhibitors play an important role on the microstructure of bulk matrix of cementitious materials, which in turn considerably influences the migration of inhibitors and chloride ions towards the surface of steel. Therefore, the combination of electrochemical tests and micro-

Table 2
The electrochemical parameters derived from CP tests.

Specimen	E_{corr} (V_{SCE})	E_{pit} (V_{SCE})	E_{rep} (V_{SCE})	i_{pass} (mA cm^{-2})	i_{max} (mA cm^{-2})
As-received					
Blank	−0.65	–	–	0.20	0.30
SN	−0.42	0.55	0.75	0.01	0.03
SP	−0.65	0.55	0.65	0.01	0.04
Pre-rusted					
Blank	−0.60	–	–	0.08	0.20
SN	−0.60	0.45	0.70	0.01	0.04
SP	−0.65	0.45	0.70	0.01	0.05

Table 3
The electrochemical indexes for pitting corrosion probability of reinforcing steel with SN and SP.

Specimen	$\Delta E_1 = E_{pit} - E_{rep}$ (V_{SCE})	$\Delta E_2 = E_{rep} - E_{corr}$ (V_{SCE})	$\Delta E_3 = E_{pit} - E_{corr}$ (V_{SCE})
As-received			
SN	−0.2	1.17	0.97
SP	−0.1	1.30	1.20
Pre-rusted			
SN	−0.25	1.30	1.05
SP	−0.25	1.35	1.10

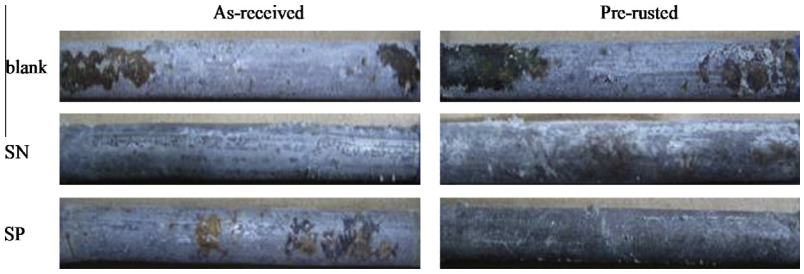

Fig. 6. Surface corrosion morphology of reinforcing steel in mortar specimens after 360 days exposure in 3.5% NaCl solution.

structural observations can be used to yield much more reasonable mechanisms of corrosion inhibition [41].

Fig. 7 depicts the SEM images of the microstructure of steel–mortar interface with and without inhibitors. It can be observed in Fig. 7a that many loose fibrous C–S–H gels and crystallized ettringite needles are formed in the blank mortar. In the presence of SN, the mortar contains more compact C–S–H gels compared to blank mortar as shown in Fig. 7b. Moreover, some macro-voids also appear with some well-developed ettringite needles, which is in close agreement with the results of Sagoe-Crentsil et al. [41]. Unlike the microstructures of blank and SN specimens, some microcracks could be observed in the bulk matrix of specimen with SP (Fig. 7c). However, no visual micropores and well-crystallized ettringite needles can be observed in the microstructure of SP specimen. Also, as suggested by Sagoe-Crentsil et al. [41], the phosphate favored the formation of lath-shaped crystals of Friedels salt which resulted in the decrease in the free chloride ions. It was reasonably inferred that phosphate interfered with the equilibrium between $Ca(OH)_2$ in mortar [13], and the formation of low solubility of $Ca_3(PO_4)_2$ precipitate were thought to fill in the air voids or microcracks in mortar [24]. However, excessive precipitates may result in the expansion and finally crack of mortar microstructure. Therefore, it would be reasonable to consider that the introduction of phosphate in cementitious materials shows a dual effect [9]: the reaction with steel against chloride ions and the formation of precipitates with the hydration products of cement, notably $Ca(OH)_2$ and C–S–H gel, as given in Eqs. (6) and (7), respectively.

$$3Fe^{2+} + 2PO_4^{3-} + 8H_2O \rightarrow Fe_3(PO_4)_2 \cdot 8H_2O \quad (6)$$

$$3Ca^{2+} + 2PO_4^{3-} \rightarrow Ca_3(PO_4)_2 \quad (7)$$

Similarly, the recent work by Bastidas et al. [19] found that the crystallization of chlorapatite ($Ca_5(PO_4)_3Cl$) and the precipitation of solid phase $FePO_4{\cdot}2H_2O$ may act as two physical barriers inhibiting steel corrosion. However, as previously mentioned, phosphate in this study may be a cathodic inhibitor, thus the inhibiting efficiency of SP is a little inferior to SN. As indicated above, it should be taken into account that the formation of $Ca_3(PO_4)_2$ precipitate plays a competitive role on the inhibiting efficiency. The depletion of effective PO_4^{3-} is thought to result in the decline of corrosion inhibition [7]. Besides, the accumulation of precipitate in the micropores of mortar matrix tends to delay the diffusion of chlorides and to improve the microstructures of steel–mortar interface.

3.6. The impact of inhibitors on the mechanical properties of mortars

Although the inhibitors are capable of delaying the time to corrosion initiation or decreasing the corrosion rate to some extent, it could not, however, neglect the influence of inhibitors on the rheological properties and mechanical properties of mortar/concrete bulk matrix [4,42]. It is found that the addition of SP in cement specimens with the same dosage of that in electrochemical tests increases the initial setting time as well as final setting time, in comparison to the blank one. This is in agreement with the previous studies [11,17,43]. It was reported that phosphates induced a retardation of cement setting due to the formation of calcium phosphate. Besides, phosphates also played an evident effect on the mechanical properties of concrete when added during mixing [17].

The mechanical properties of mortar specimens with and without SN and SP inhibitors were acquired experimentally at the age of 28 and 360 days as shown in Fig. 8. It is clear from Fig. 8a that 28 d flexural strength (f_t) of specimens with SN and SP is slightly lower than the blank specimen (without inhibitors). However, after long-term exposure to atmospheric environment, the 360 d f_t values of specimens with SN and SP increase to a greater extent than the blank specimen. And there is no clear distinction of 360 d f_t values has been found between SP and blank specimens. It is worth noting, therefore, that the 360 d f_t value of SN specimen is higher than blank and SP specimens, whereas SP specimen shows similar value with blank specimen.

Fig. 8b presents the 28 d and 360 d compressive strength (f_c) of mortar specimens. It is evident that the f_c values of SN specimens are higher than blank specimens, regardless of 28 d and 360 d. Nevertheless, the 28 d f_c value of SP specimen is somewhat lower in comparison to blank specimen, although both mortar specimens exhibit almost the same 360 d f_c values. The results of mechanical properties are in good agreement with the investigations conducted by Thomas [43]; it revealed that NO_2^- was a strong cement accelerator, while PO_4^{3-} seemed to be a relatively weak cement retarder.

Based on the results of f_t and f_c values at 360 d, it is found that the nitrites tend to be a strength enhancer, while phosphates seem to exert little effect on the development of strength of mortars. It is

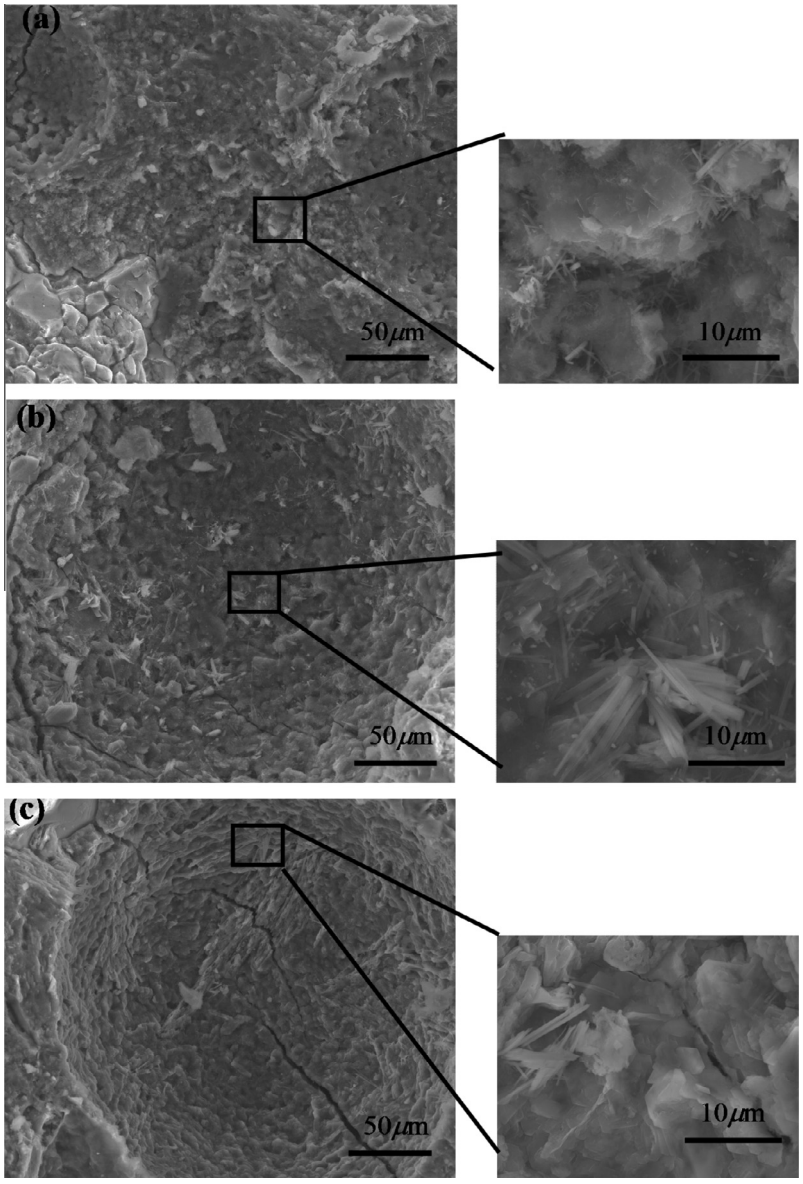

Fig. 7. The effect of inhibitors on the microstructure of as-received mortar specimens exposed in 3.5% NaCl solution for 360 days. (a) Blank; (b) SN and (c) SP.

important to recognize, however, that the mechanical properties of mortar specimens with SN or SP significantly depend on the dosage of inhibitors. Therefore, optimum dosage of inhibitors should be obtained concerning both the mechanical properties and inhibiting efficiency, which is a matter for further investigation.

4. Conclusion

As is demonstrated, the combination of electrochemical measurements, microstructural characterization and mechanical property tests is suitable to assess the inhibiting efficiency and to reveal the inhibition mechanism of corrosion inhibitors in mortars. The following conclusions can be drawn from this work:

1. When the dosage is 0.4 mol in 1 kg cement, nitrite is indicated as an anodic inhibitor according to the reduced corrosion rate and more noble E_{corr} value. At the same concentration, phosphate can also decrease the corrosion rate but with more negative E_{corr} value, which indicates that phosphate might be a cathodic inhibitor.
2. The results of LPR and EIS indicate that, at the same concentration by the weight of cement, nitrite is thought to be more effective to reduce the uniform corrosion rate of reinforcing steel than phosphate. However, the probability of pitting corrosion is slightly lower for the specimens containing phosphate, relative to those containing nitrite, according to the results of cyclic polarization tests.
3. Comparing to as-received steels, the pre-rusted steels show slightly higher uniform corrosion rate. Furthermore, the probability of pitting corrosion is almost the same for both cases. This is attributed to the uniform corrosion products and white deposits formed on the surface of pre-rusted steels which can prevent the further attack of chloride ions.
4. Phosphate in cementitious materials shows a dual effect: the reaction with steel against chloride-induced corrosion, and the formation of precipitates with hydration products of cement. The precipitates of $Ca_3(PO_4)_2$ accumulated in the micropores and microcracks of mortar matrix and steel–mortar interface could on the one hand delay the diffusion of detrimental substances (Cl^-, O_2 and H_2O, etc.). However, the depletion of

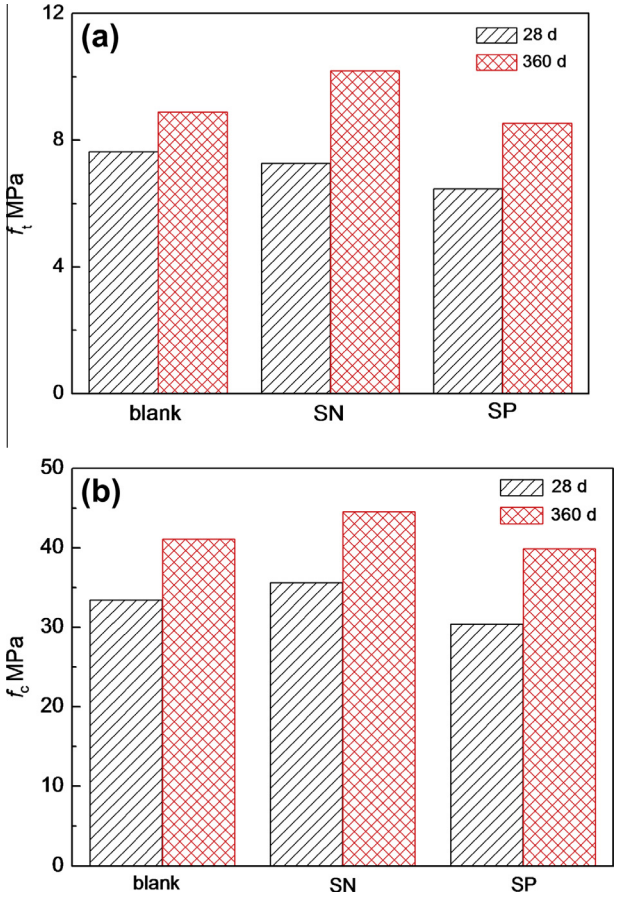

Fig. 8. The effects of SN and SP on the mechanical properties of mortar specimens. (a) Flexural strength f_t and (b) compressive strength f_c.

PO_4^{3-}, which is the effective constituent of phosphates, may result in the partial loss of its long-term effectiveness on the other hand.

5. Although the mortar specimens with phosphate show relatively increased setting time and lower early mechanical properties, it has been confirmed that phosphate has little effect on the long-term mechanical properties of mortars.

Acknowledgments

The authors greatly acknowledge support provided by the National Basic Research Program of China (No. 2009CB623203), the National High Technology Research and Development Program of China (No. 2008AA030704), and the National Natural Science Foundation of China (No. 51208098). The authors are also grateful to Dr. C. Yu for assistance with the English presentation of this research.

References

[1] Kim CY, Kim JK. Numerical analysis of localized steel corrosion in concrete. Constr Build Mater 2008;22:1129–36.
[2] Soylev TA, Richardson MG. Corrosion inhibitors for steel in concrete: state-of-the-art report. Constr Build Mater 2008;22:609–22.
[3] Lee HS, Shin SW. Evaluation on the effect of lithium nitrite corrosion inhibitor by the corrosion sensors embedded in mortar. Constr Build Mater 2007;21:1–6.
[4] Justnes H. Corrosion inhibitors for reinforced concrete. ACI SP 2006;234–04:53–70.
[5] Østnor TA, Justnes H. Anodic corrosion inhibitors against chloride induced corrosion of concrete rebars. Corros Eng Sci Technol 2011;110:131–6.
[6] Valcarce MB, Vazquez M. Phosphate ions used as green inhibitor against copper corrosion in tap water. Corros Sci 2010;52:1413–20.
[7] Andrade C, Alonso C, Acha M, Malric B. Preliminary testing of Na_2PO_3F as a curative corrosion inhibitor for steel reinforcements in concrete. Cem Concr Res 1992;22:869–81.
[8] Douche-Portanguen A, Prince W, Lutz T, Arliguie G. Detection or quantitative analysis of a corrosion inhibitor, the sodium monofluorophosphate, in concrete. Cem Concr Compos 2005;27:679–87.
[9] Reffass M, Sabot R, Jeannin M, Berziou C, Refait P. Effects of phosphate species on localised corrosion of steel in $NaHCO_3$ + NaCl electrolytes. Electrochimi Acta 2009;54:4389–96.
[10] Abd El Haleem SM, Abd El Wanees S, Abd El Aal EE, Diab A. Environmental factors affecting the corrosion behavior of reinforcing steel II Role of some anions in the initiation and inhibition of pitting corrosion of steel in $Ca(OH)_2$ solutions. Corros Sci 2010;52:292–302.
[11] Jin SX, Sagoe-Crentsil KK, Glasser FP. Characteristics of corrosion inhibition admixtures in OPC paste with chloride additions Part I: Chemistry and electrochemistry. Mag Concr Res 1991;43:205–13.
[12] Dhouibi L, Triki E, Raharinaivo A, Trabanelli G, Zucchi F. Electrochemical methods for evaluating inhibitors of steel corrosion in concrete. Br Corros J 2000;35:145–9.
[13] Dhouibi L, Triki E, Salta E, Rodrigues P, Raharinaivo A. Studies on corrosion inhibition of steel reinforcement by phosphate and nitrite. Mater Struct 2003;36:530–40.
[14] Etteyeb N, Sanchez M, Dhouibi L, Alonso C, Andrade C, Triki E. Corrosion protection of steel reinforcement by a pretreatment in phosphate solutions: assessment of passivity by electrochemical techniques. Corros Eng Sci Technol 2006;41:336–41.
[15] Etteyeb N, Dhouibi L, Sanchez M, Alonso C, Andrade C, Triki E. Electrochemical study of corrosion inhibition of steel reinforcement in alkaline solutions containing phosphates based components. J Mater Sci 2007;42:4721–30.
[16] Etteyeb N, Dhouibi L, Takenouti H, Alonso MC, Triki E. Corrosion inhibition of carbon steel in alkaline chloride media by Na_3PO_4. Electrochimi Acta 2007;52:7506–12.
[17] Etteyeb N, Sanchez M, Dhouibi L, Alonso MC, Takenouti H, Triki E. Effectiveness of pretreatment method to hinder rebar corrosion in concrete. Corros Eng Sci Technol 2010;45:435–41.
[18] Génin JMR, Dhouibi L, Refait P, Abdelmoula M, Triki E. Influence of phosphate on corrosion products of iron in chloride-polluted-concrete-simulating solutions: ferrihydrite vs green rust. Corrosion 2002;58:467–78.
[19] Bastidas DM, La Iglesia VM, Criado M, Fajardo S, La Iglesia A, Bastidas JM. A prediction study of hydroxyapatite entrapment ability in concrete. Constr Build Mater 2010;24:2646–9.
[20] Bastidas DM, Criado M, La Iglesia VM, Fajardo S, La Iglesia A, Bastidas JM. Comparative study of three sodium phosphates as corrosion inhibitors for steel reinforcements. Cem Concr Compos 2013;43:31–8.
[21] Poursaee A, Hansson CM. Potential pitfalls in assessing chloride-induced corrosion of steel in concrete. Cem Concr Res 2009;39:391–400.
[22] Hansson CM, Mammoliti L, Hope BB. Corrosion inhibitors in concrete – Part I: The principles. Cem Concr Res 1998;28:1775–81.
[23] Soeda K, Ichimura T. Present state of corrosion inhibitors in Japan. Cem Concr Compos 2003;25:117–22.
[24] Jang JW, Hagen MG, Engstrom GM, Iwasaki I. Cl^-, SO_4^{2-}, and PO_4^{3-} distribution in concrete slabs ponded by corrosion-inhibitor-added deicing salts. Adv Cem Based Mater 1998;8:101–7.
[25] Montemor MF, Simoes AMP, Ferreira MGS. Chloride-induced corrosion on reinforcing steel: from the fundamentals to the monitoring techniques. Cem Concr Compos 2003;25:491–502.
[26] Vedalakshmi R, Saraswathy V, Song HW, Palaniswamy N. Determination of diffusion coefficient of chloride in concrete using Warburg diffusion coefficient. Corros Sci 2009;51:1299–307.
[27] Eichler T, Isecke B, Baßler R. Investigations on the re-passivation of carbon steel in chloride containing concrete in consequence of cathodic polarisation. Mater Corros 2009;60:119–29.
[28] Vedalakshmi R, Palaniswamy N. Analysis of the electrochemical phenomenon at the rebar–concrete interface using the electrochemical impedance spectroscopic technique. Mag Concr Res 2010;62:177–89.
[29] Koleva DA, de Wit JHW, van Breugel K, Lodhi ZF, van Westing E. Investigation of corrosion and cathodic protection in reinforced concrete I. Application of electrochemical techniques. J Electrochem Soc 2007;154:P52–61.
[30] Pradhan B, Bhattacharjee B. Performance evaluation of rebar in chloride contaminated concrete by corrosion rate. Constr Build Mater 2009;23:2346–56.
[31] Ghods P, Isgor OB, McRae GA, Gu GP. Electrochemical investigation of chloride-induced depassivation of black steel rebar under simulated service conditions. Corros Sci 2010;52:1649–59.
[32] Saremi M, Mahallati E. A study on chloride-induced depassivation of mild steel in simulated concrete pore solution. Cem Concr Res 2002;32:1915–21.
[33] Alonso-Falleiros N, Hakim A, Wolynec S. Comparison between potentiodynamic and potentiostatic tests for pitting potential measurement of duplex stainless steels. Corrosion 1999;55:443–8.
[34] Li L, Sagüés AA. Chloride corrosion threshold of reinforcing steel in alkaline solutions—cyclic polarization behavior. Corrosion 2002;58:305–16.
[35] Troconis de Rincon O, Perez O, Paredes E, Caldera Y, Urdaneta C, Sandoval I. Long-term performance of ZnO as a rebar corrosion inhibitor. Cem Concr Compos 2002;24:79–87.

[36] García-Alonso MC, Escudero ML, Miranda JM, Vega MI, Capilla F, Correia MJ, et al. Corrosion behaviour of new stainless steels reinforcing bars embedded in concrete. Cem Concr Res 2007;37:1463–71.
[37] Refaey SAM, Abd El-Rehim SS, Taha F, Saleh MB, Ahmed RA. Inhibition of chloride localized corrosion of mild steel by PO_4^{3-}, CrO_4^{2-}, MoO_4^{2-}, and NO_2^- anions. Appl Surf Sci 2000;158:190–6.
[38] Sagoe-Crentsil KK, Glasser FP. Constitution of green rust and its significance to the corrosion of steel in Portland cement. Corrosion 1993;49:457–63.
[39] Koleva DA, de Wit JHW, van Breugel K, Lodhi ZF, Ye G. Investigation of corrosion and cathodic protection in reinforced concrete II. Properties of steel surface layers. J Electrochem Soc 2007;154:C261–71.
[40] Al-Tayyib AJ, Khan MS, Allam IM, Al-Mana AI. Corrosion behavior of pre-rusted rebars after placement in concrete. Cem Concr Res 1990;20:955–60.
[41] Sagoe-Crentsil KK, Jin SX, Glasser FP. Characteristics of corrosion inhibition admixtures in OPC paste with chloride additions Part II: Microstructures and mechanisms. Mag Concr Res 1991;43:275–80.
[42] De Schutter G, Luo L. Effect of corrosion inhibiting admixtures on concrete properties. Constr Build Mater 2004;18:483–9.
[43] Thomas NL. Corrosion problems in reinforced concrete: why accelerators of cement hydration usually promote corrosion of steel. J Mater Sci 1987;22:3328–34.